www.czasopisma.pan.pl PAN POLSKA AKADEMIA NAUK www.journals.pan.pl

Arch. Metall. Mater. **66** (2021), 1, 65-72

DOI: 10.24425/amm.2021.134760

D. BOLIBRUCHOVÁ[1], M. KURIŠ[1*], M. MATEJKA[1], K. MAJOR GABRYŚ[2], M. VICEN[3]

EFFECT OF Ti ON SELECTED PROPERTIES OF AlSi7Mg0.3Cu0.5 ALLOY WITH CONSTANT ADDITION OF Zr

The article is focused on the synergic effect of constant content of Zr and higher content of Ti on mechanical properties Al-Si alloy. The Ti additions were in proportions of 0.1, 0.2 and 0.3 wt.% Ti. The casting process was carried out in ceramic molds, created for the investment casting technology. Half of the experimental samples were processed by precipitation curing T6. The measured results were compared with primary alloy AlSi7Mg0,3 and experimental alloy AlSi7Mg0.3Cu0.5Zr0.15. In variant with addition 0.1 wt. %, the tensile strength R_m increased by 1,5% but the elongation A_M decreased to 40%. Variants with 0.2 and 0.3 wt. % addition of Ti achieved similar R_m but approximately 40% decrease in A_M. However, it is interesting that yield strength $R_{p0.2}$ increased for all variants by approximately 14 to 20%. The results point out the possibility of developing a more sophisticated alloy for automotive industry.

Keywords: AlSi7Mg0.3Cu0.5, Investment casting, Zirconium, Titanium, Increasing mechanical properties

1. Introduction

The automotive and aerospace industries require a constant need to improve the properties of the materials originally used. The development in the given field includes also Al alloys, but focuses on improving not only their mechanical properties but also the heat resistance of Al alloys in applications above 250°C. Prominent representatives of such improvements are the castings of cylinder heads, gearboxes and engine blocks. Here the emphasis is on the lowest casting weight possible and the ability to function at high performance and temperatures. The application of a more sophisticated alloy with improved mechanical properties and heat resistance increases material savings by reducing the dimensions of engine blocks, improving the environmental aspect by reducing fuel consumption, and increasing performance due to the improved resistance of Al castings to operating pressures and heat load during the device operation (Fig. 1) [1-10].

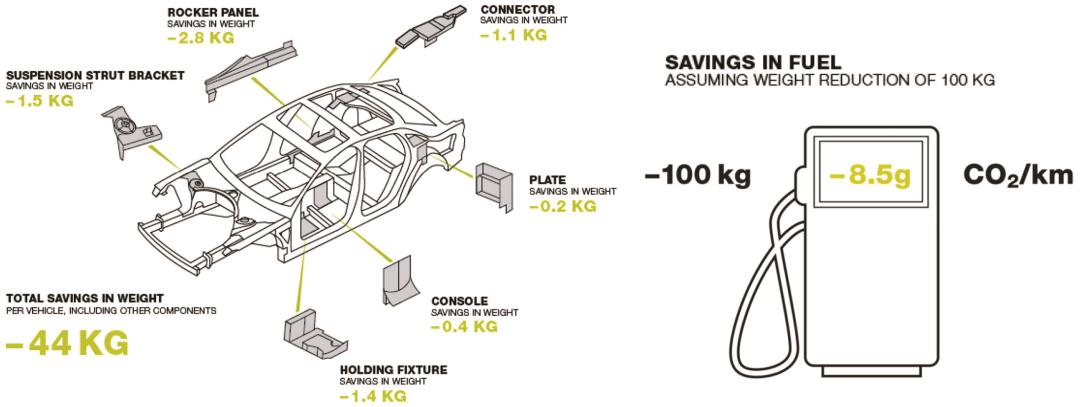

Fig. 1. Effect of lightening the components on reducing CO_2 greenhouse gas [5]

[1] UNIVERSITY OF ŽILINA, FACULTY OF MECHANICAL ENGINEERING, DEPARTMENT OF TECHNOLOGICAL ENGINEERING, ŽILINA, SLOVAKIA
[2] AGH UNIVERSITY OF SCIENCE AND TECHNOLOGY, FACULTY OF FOUNDRY ENGINEERING, DEPARTMENT OF MOULDING MATERIALS, MOULD TECHNOLOGY AND NON-FERROUS METALS CASTING, AL. MICKIEWICZA 30,30-059 KRAKÓW, POLAND
[3] UNIVERSITY OF ŽILINA, FACULTY OF MECHANICAL ENGINEERING, DEPARTMENT OF MATERIAL ENGINEERING, ŽILINA, SLOVAKIA

* Corresponding author: michal.kuris@fstroj.uniza.sk

The AlSi7Mg0.3 Al alloy is frequently used in the manufacture of castings where good casting properties, corrosion resistance, pressure tightness and weldability are required. It is therefore often used in the manufacture of components for internal combustion engines. Improvement of the strength properties of the AlSi7Mg0.3 Al alloy can be ensured by the addition of various elements, with copper being particularly important. The addition of Cu provides increased strength, hardness or creep resistance by eliminating the curable Al_2Cu phases. These can be precipitated either as small oval grains with a high Cu concentration or as a ternary Al-CuAl2-Si eutectic. However, increasing Cu content in the AlSi7Mg0.3 Al alloy decreases ductility, adversely affects corrosion resistance and increases solidification interval. The combination of Mg and Cu allowed the development of commercial alloys such as AlSi7MgCu0.5, AlSi8Cu3 and AlSi7Mg0.3Cu. The AlSi7Mg0.3Cu alloy is the one used most frequently in the manufacture of components for internal combustion engines. The main characteristic of the above-mentioned alloys is the crystallization of two eutectics: primary Al-Si and secondary Al-Si-Cu. The introduction of Zr into the alloy is important in order to increase the strength, while the strengthening effect is induced by the elimination of the Al_3Zr or AlSiZr intermetallic phases. Primarily, Zr is precipitated in the form of Al_3Zr during the peritectic reaction, with a Zr content of ≥0.1 wt.%. The Al_3Zr phase is has two different crystallographic morphologies. The first is the tetragonal DO_{23} system, the second is the cubic coherent metastable $L1_2$ system (Fig. 2) [8-21].

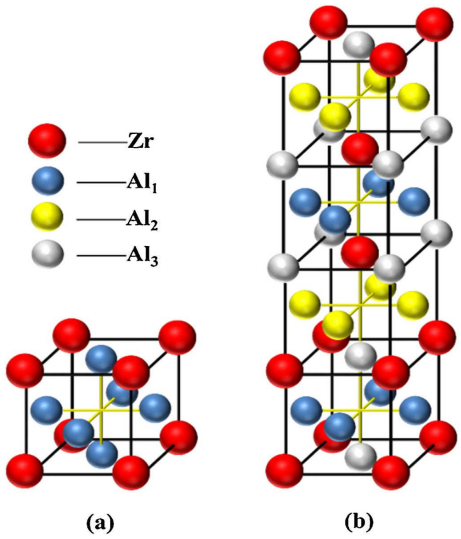

Fig. 2. Al_3Zr phase crystallographic lattices: a) $L1_2$ b) DO_{23} [4]

Zr is characterized by the lowest diffusion in Al compared to other elements such as Mn, V or Sc. Zr atoms have high binding energy with unoccupied Al sites. The Al_3Zr particles are resistant to dissolution and roughening, they regulate the development of grains and sub-grains in the metal matrix of the Al-Si alloy. This makes it possible to increase and maintain the strength of the Al alloy even after precipitation hardening, above 250°C. DO_{22} and DO_{23} tetragonal lattices influence the strength characteristics of construction materials. However, these phases are too fragile due to the low symmetry of the tetragonal lattice. A more preferred variant is the $L1_2$ cubic lattice, which better compensates for the negative aspect of the DO_{22} and DO_{23} tetragonal lattices. The Al_3Zr intermetallic phases in an Al-Si-based alloy can be evolved either in long acicular (needle-like) form or in a square-like (angular) form. Zr can positively influence the properties of Al-Si alloys, therefore the more advantageous is the combination of Zr with other elements such as Ti, Sr, Sc, Mo or lanthanides. As confirmed by the work of Nabawy and Voncina [8-9], Ti in combination with Zr can induce primary grain and sub-grain refinement in an Al alloy. Ti has a significant inoculation effect on the alloy under investigation. It also causes an increase in the number of nuclei for the Al_3Zr phase at a higher Ti content. At a higher Ti content it replaces the Zr atoms in the Al_3Zr phase, thereby enhancing the smoothening and strengthening effect on the Al alloy. At temperatures above 300°C, phases with a higher Ti content are characterized by increased stability. Intermetallic phases containing Zr and Ti provide higher resistance and strengthening characteristics than Al_2Cu or Mg_2Si phases, which become unstable at temperatures above 250°C. The market growth and demand for electric vehicles (EV) also have a significant impact on Al casting manufacturers. The main focus is on the possibility of producing low-weight components that allow less power consumption from battery cells and thus increase EV range on a single charge. At the same time, highly favourable mechanical properties combined with high corrosion resistance, electrical permeability and resistance to higher temperatures represent a very interesting material in the construction of modern EVs [8-26].

2. Methods and goals

The aim of the experiments was to determine the impact of the synergistic effect of Zr and Ti on selected properties of the AlSi7Mg0.3Cu alloy which was cast by investment casting technology. The ceramic mold consists of three layers ensuring the formation of a contact, insulating and reinforcing cover (Table 1). After melting and cooling for at least 24 hours the ceramic mold (Fig. 3a) of approximately 3 mm thickness was annealed at 750°C for at least 1.5 hours. The ceramic mold tem-

TABLE 1

Ceramic mold material composition [4]

Component	1. Layer	2. Layer	3. Layer	4. Layer	5. Layer
Binder	Primcot cote plus	SP-Ultra 2408	MatriXsol 30	MatriXsol 30	MatriXsol 30
Grain	Cerabed DS 60	Rancosil A	Molochite 30-80 DD	Molochite 30-80 DD	Molochite 30-80 DD

perature was 510-540°C before casting. The samples were cast at a rate of 0.3 kg/s from a casting height of 500 mm.

The casting temperature was 750 ± 10°C. Ti was inserted in to the melt AlSi7Mg0,3Cu alloy in form of AlTi5B master alloy. The master alloy AlTi5B was crushed into smaller pieces, about size 0.5 until 1 cm, and taken into the melt for 30 minutes. After this time the melt was mixture and cast into the ceramic mould. After casting, the ceramic mold was cooled on air for one hour. The AlSi7Mg0.3Cu primary alloy was supplied in a pre-inoculated and pre-modified condition. The AlSi7Mg0.3Cu alloy represents a new type of alloys not standardized according to STN EN 1706 (Table 2).

A total of 3 experimental melts were prepared, characterized by a constant Zr content of 0.15 wt.% and a gradual addition of Ti by 0.1 wt.%. The AlSi7Mg0.3Cu experimental alloys were not degassed or refined throughout the experiment. The AlZr15 master alloy featured impaired melt solubility. After casting the experimental samples with a constant addition of 0.15 wt.% Zr and a gradual addition of Ti in the range of 0.1 to 0.3 wt.% (Table 2), the process was followed by heat treatment ("HT") in the form of T6 precipitation curing. HT was performed on 5 pcs of a total of 10 experimental samples (Fig. 3b) from each experimental variant. Subsequently, the individual samples were evaluated for mechanical properties before and after the HT process, whereby the arithmetic mean was determined from the mechanical characteristics and a graph was made for each experimental variant. The highest mechanical characteristic values obtained were selected in order to evaluate the microstructure before and after HT. For the Zr-phase distinguishability and unmistakability, these samples were etched with a ferric-phase etch (H_2SO_4). Primarily, the results of the mechanical properties were confronted with the values of the AlSi7Mg0.3Cu primary alloy ("P alloy"), and the AlSi7Mg0.3CuZr0.15 reference alloy ("R alloy"). The R alloy represents an alloy with the most preferred addition of Zr. In the above-mentioned alloy, an optimum increase of selected mechanical properties such as $Rp_{0.2}$, E or HBW was observed for the alloy in the alloying range from 0.05 wt.% to 0.3 wt.% Zr.

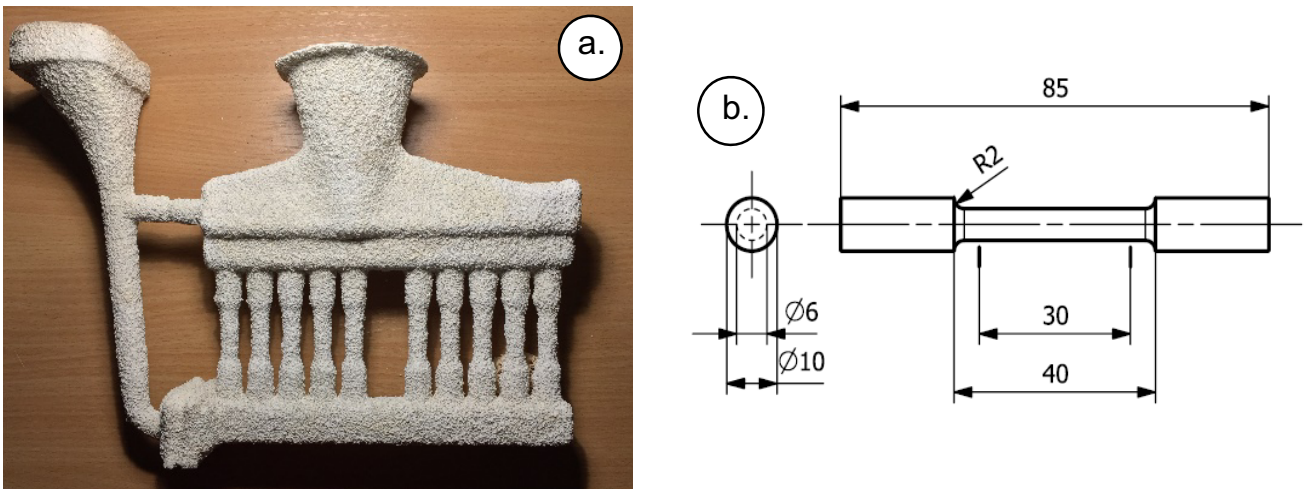

Fig. 3. a) Ceramic mold supplied by AluCAST, b) Scheme of the test specimen [4]

TABLE 2

Chemical composition of P, R, E1, E2 and E3 alloys

Variant	Si	Fe	Cu	Mn	Mg	Zn	Ti	Zr	Al
P	6.88	0.12	0.54	0.07	0.37	0.07	0.13	-	rest
R	6.86	0.12	0.55	0.07	0.37	0.07	0.13	0.15	rest
E1	6.96	0.13	0.55	0.07	0.37	0.01	0.23	0.12	rest
E2	6.68	0.13	0.54	0.07	0.35	0.01	0.28	0.14	rest
E3	6.51	0.13	0.52	0.07	0.34	0.01	0.37	0.13	rest

P – chemical composition of AlSi7Mg0.3Cu alloy; R – reference alloy AlSi7Mg0.3Cu with addition of Zr 0,15 wt. %;
E1, E2, E3 – experimental alloys AlSi7Mg0.3Cu with constant addition of Zr 0.15 hm. % and gradual increasing of Ti o 0.1 wt. %

TABLE 3

Temperatures of structural components formation in E1, E2, E3 and R alloys

Variant	0.15 wt.% Zr	0.1 wt.% Ti	0.2 wt.% Ti	0.3 wt.% Ti
α phase (°C)	619	617	623	613
Eutectic (°C)	563	556	565	560
Zr phase (°C)	630	—	634	626

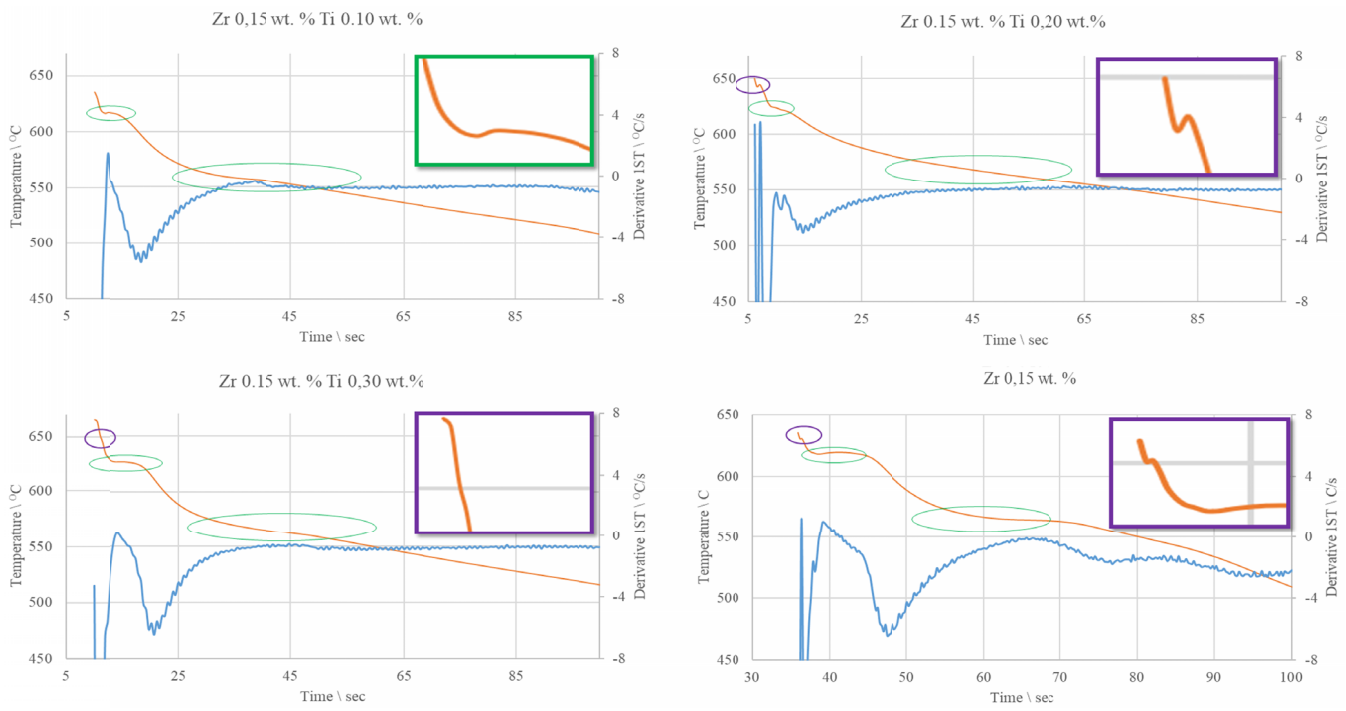

Fig. 4. Cooling curves and derived curves of experimental E1, E2, E3 and R alloys

3. Results and discussion

The evaluation of thermal analysis revealed differences in the area of Zr phase separation (elimination) in samples with addition of Ti versus the R alloy (Fig. 4). The α-phase separation occurs in the combination of Zr and Ti in the temperature range of 613 to 621°C (Table 3).

The eutectic is formed at temperatures of about 556 to 565°C. On the basis of the derived cooling curves (Fig. 4), we observed the formation of the curable Mg_2Si phases as well, at temperatures of 550 to 555°C. Purple ellipses indicate the formation of predicted Zr phases in the temperature range of 626 to 634°C. At the given position we can assume formation of Zr phases that were confirmed at a later evaluation of their microstructure (Fig. 9). Based on the values obtained we can assume that the Zr phases are formed even before the α-phase and the eutectic. In experimental alloys with an addition of Ti 0.1 wt.% and 0.3 wt.% there is no higher level of super-cooling compared to the R alloy with an addition of 0.15 wt.% Zr. A partial change compared to the R alloy occurs in the variant with an addition of 0.2 wt.% Ti. Mechanical characteristics are improved with an increase in Ti addition, which in many cases exceed the best measured results in experimental alloys alloyed only using Zr. From the viewpoint of evaluating the tensile strength R_m (Fig. 5) before HT, the E1 experimental samples achieved the best results.

Before HT, the E1 samples reached R_m of about 167 MPa, which represents a lower value compared to the P samples by 2% and compared to the R alloy by 3%. After HT, samples of E1 again made the best values, reaching 264 MPa. The given value is significant precisely because the previous samples, with the addition

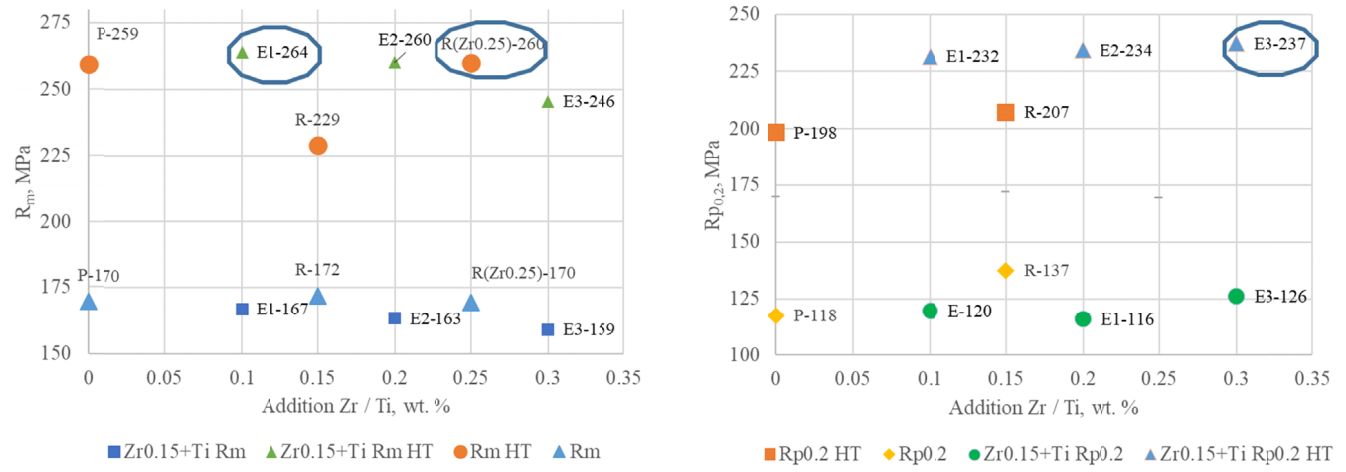

Fig. 5. Dependence of R_m and $Rp_{0.2}$ before and after HT for investigation alloys AlSi7Mg0.3Cu

of only Zr, reached the highest value up to 260 MPa. This value is considered by the STN EN 1706 standard to be the minimum R_m value of the AlSi7Mg0.3 alloy. The E1 samples reached a R_m value that is 2% higher than that of the P alloy, and 2% higher than that of the R alloy. The best results of the agreed $Rp_{0.2}$ yield strength were achieved by the E3 sample with an addition of 0.3 wt.% Ti (Fig. 5). The increase achieved was by 20% compared to the P alloy and 15% compared to the R alloy witch was the best alloy variant with only Zr addition. Increased plasticity during engine operation ensures better adaptation of the cylinder head to temperature changes and operating pressure exerted during operation, thus extending the service life. Positive results, similar to $Rp_{0.2}$, were also measured at the E – modulus of elasticity (Fig. 6).

Best results were obtained in the case of E3 samples with a constant addition of 0.15 wt.% Zr and 0.3 wt.% Ti. Compared to the P alloy, the increase in E is up to 21%, and compared to the R alloy it is by up to 18%. The best experimental alloy with a constant addition of 0.2 wt.% Zr achieves approximately 10% lower E than the E3 experimental alloy. Based on the given parameters we can conclude that the examined samples are able to withstand higher operating loads during the device operation. By increasing $Rp_{0.2}$ and E we obtained an AlSi7Mg0.3Cu alloy, which is able to withstand the same or, eventually, higher operating loads even when the functional cross-sections of the casting walls (e.g. cylinder heads) are narrowed. Of all the mechanical properties, a decrease was observed at ductility A (Fig. 6). In contrast to the P alloy, the results of the A alloy are slightly better than those of the R alloy with an addition of 0.15 wt.% Zr. Although the E3 samples with the addition of 0.3 wt.% Ti reach lower values before HT by 30% and after HT by 13%, other variants E1 and E2 achieved a significant improvement in ductility. For E1 experimental samples, this is an increase by 23% before HT and by almost 50% after HT. The E2 samples achieved an improvement of 15% before and after HT similar to E1 up to 50%. The significance of ductility (elongation) is especially important for the motor parts of the engine during its operation. In the case of reduced ductility, some components such as e.g. the engine cylinders could not react flexibly and plastically enough to the desired extent during the temperature change in the combustion chamber. This would reduce the service life of any internal combustion engine. When evaluating the hardness, its increase compared to the P alloy was between 9 and 15%, and compared to the R alloy the value was between 6 and 12% (Fig. 7). The best values were obtained from E3 experimental samples with a value achieved of 102 HBW. The increase compared to the P alloy is by 15%, compared to the R alloy by 12%,

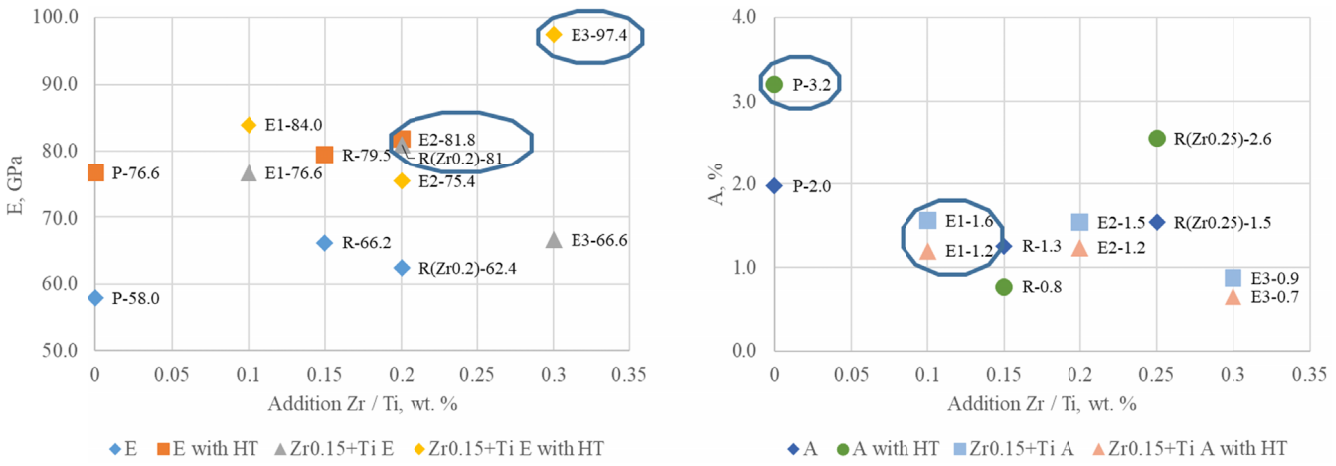

Fig. 6. Dependency of E and A before and after HT for investigation alloys AlSi7Mg0.3Cu

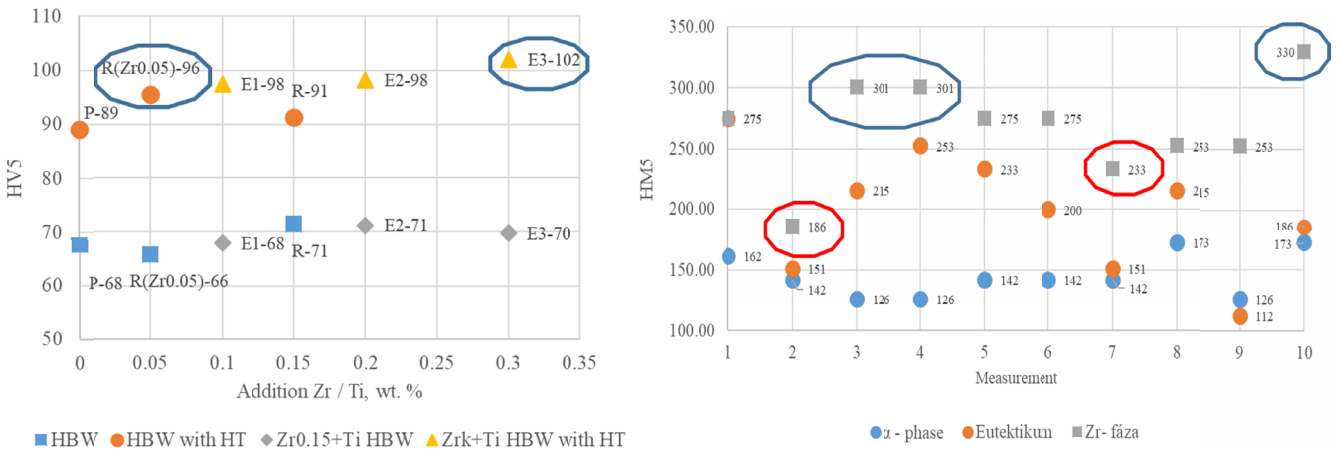

Fig. 7. HBW for investigation alloys AlSi7Mg0.3Cu and HM5 microhardness for E3 alloy

and compared to the best experimental variant with an addition of Zr 0.05% by 7%. However, a positive increase is noticeable in all experimental alloys with a combination of Zr and Ti. The microhardness of the Zr phases was evaluated as the arithmetic mean of the 10 test punctures, reaching a value of about 265 HM5 achieved by the E3 experimental samples (Fig. 7). The microhardness of Zr phases is between the hardness of Al_4Ca and Al_6CuMg phases, which are characterized by microhardness in the range of 200 to 300 HM5.

In the evaluation of microhardness, a decrease was observed in Zr phases in interaction with other phases, e.g. on Mg or Fe base (Fig. 7). This can be seen with punctures 3, 4 and 10, which were performed into Zr phases without interaction with other phases. In contrast, punctures 2 and 7 were performed in Zr phases in strong interaction with other phases. A similar phenomenon was observed in experimental alloys with the addition of only Zr. In metallographic evaluation, the experimental AlSi7Mg0.3Cu alloy can be defined as a sub-eutectic alloy containing primary α-phase dendrites and globular eutectic consisting of α-phase and Si. In addition to the base phases, it also contains the curing phases Mg_2S and Al_2Cu. Based on the content of elements in the alloys such as Fe and Mn, there can occur their separation in the form of ferric intermetallic phases in various morphological shapes. The effect on the resulting structure is closely related to the chemical composition and casting technology. In the mold casting technology, a quicker cooling and the formation of a fine dendritic structure can be expected, as opposed to the investment casting technology, which is characterized by much slower heat dissipation. Because the alloy is pre-modified, the acicular morphology of eutectic Si is transformed into a finer, globular morphology. Zr is formed in the metal matrix as Zr phases in the shape of longer needles with a smooth surface and cleaved ends, respectively it occurs in a more compact shorter morphology without cleaved ends. The Zr phases observed on microstructures are intermetallic phases of the Al_3Zr and AlSiZr type. Similar phase morphology is identified by Vončina in his work [9]. Zr is characterized by the least diffusion to the α matrix and is therefore formed preferably as Al_3Zr. From previous experiments it was found that Zr phases bind not only Fe, thus suppressing the negative effect of Fe-based phases in the metal matrix of the experimental AlSi7Mg0.3Cu alloy, but also increase the interaction with Mg_2Si phases (Fig. 8). A high presence of Ti in the respective Zr phases was found after evaluation by EDX analysis. The above-mentioned facts suggest that Ti can form nucleation sites for the Zr phase precipitation and increase their stability in the metal matrix. When comparing the E1, E2, and E3 sample microstructure with the R alloy it can be concluded that the amount of precipitated Zr phases has increased (Fig. 9). This phenomenon doubles with increasing Ti content in the alloy under investigation compared to the R alloy (Fig. 9a). When evaluating the microstructure, we can observe a uniform ratio of precipitating Zr phases in the form of longer acicular morphology with a sharp edge ending and more consistent angular morphology.

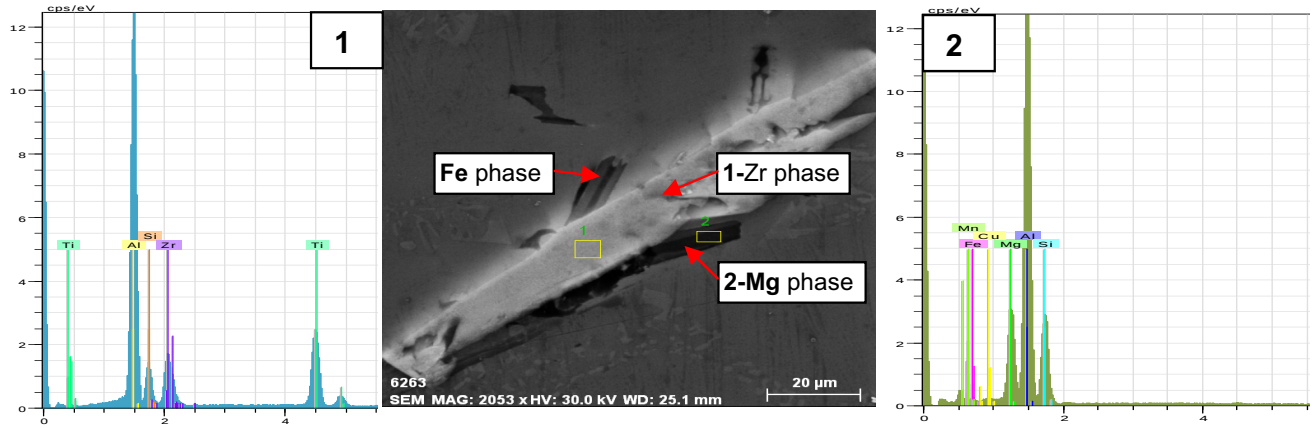

Fig. 8. EDX analysis of the Zr phase in the AlSi7Mg0.3CuZr0.15 R alloy

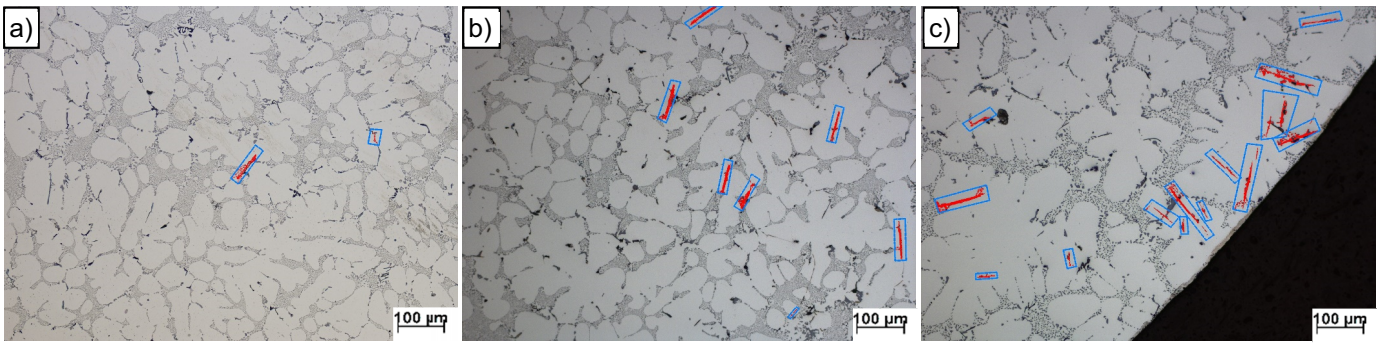

Fig. 9. Microstructure of the alloys before HT: a) R alloy, b) E1 alloy, c) E2 alloy, H_2SO_4 etch

The Zr phases were precipitated in some cases in the form of large structures in the eutectic region (Fig. 10a, 10d), or at an increased concentration of Zr phases in the subsurface region of the sample under investigation (Fig. 9c). After exceeding the Ti content ≥0.25 wt.% in the experimental samples, there was a sharp increase in the amount of precipitated Zr phases, with the preferential elimination being mainly in the subsurface area of the investigated sample. This condition is probably related to the slow cooling of the alloy in ceramic molds. At the same time, with the increased Ti content represented by samples E2 and E3, Zr phases were formed with presumed Cu enrichment (Fig. 10b, 10e). The Zr phases of acicular morphology can be observed in samples E3 (Fig. 10c, 10f). HT caused partial breakdown of larger Zr phases in acicular morphology. All samples after HT show a slight increase of R_m and a significant increase of $Rp_{0.2}$ and E. The finer, evenly distributed Zr phases act in the experimental AlSi7Mg0.3Cu alloy samples as an reinforcing element (Fig. 10g, 10h, 10i).

In contrast to the R alloy, the Zr phases were precipitated in the form of long acicular-shaped formations and consequently more pronounced disintegration after HT. The microstructures in Figs 9 and 10 show that size of the a-phase is basically unchanged though the investigated alloy contains significant additions of Ti and Zr, which are known as effective structure refiners of Al-base alloys, when they are present in melt separately. Considering the role of Ti – it is well known that it causes grain refinement of Al and most of the Al alloys. Namely, Ti provides Al_3Ti nucleant particles – substrates of heterogeneous nucleation of α(Al) solid solution [19]. It is well known that for particles to be effective nucleants, they should have surfaces with in-plane interatomic distances closely matching those in the solid to be nucleated. The Al_3Ti phase has tetragonal DO_{22} crystal structure, in which the nearest-neighbour atomic distance in {1 1 2} plane is 0.2826 nm, while in {1 1 1} plane of α(Al) it is 0.2859 nm. The very low lattice misfit in the relevant contacting planes explains the refining performance in Al and Al-alloys [20]. Furthermore, Ti in solution has strong solute effect on growth and refinement of the α(Al) phase [21]. Both these effects can contribute to significant Al matrix refinement of the mentioned alloys. Considering the role of Zr – the particles of Al_3Zr phase can also serve as the nucleant ones because their average interatomic distance in {1 1 4} plane is 0.291 nm, i.e. differs only by 1.7% from that of Al. However, the simultaneous presence of Ti and Zr in Al melt strongly decreases the refinement performance observed when they are present separately [22]. Al of commercial purity used in production of its cast or wrought alloys contains some amount of solute impurities, e.g. Fe, which can contribute to the GRF (growth restriction factor). Zirconium presence can

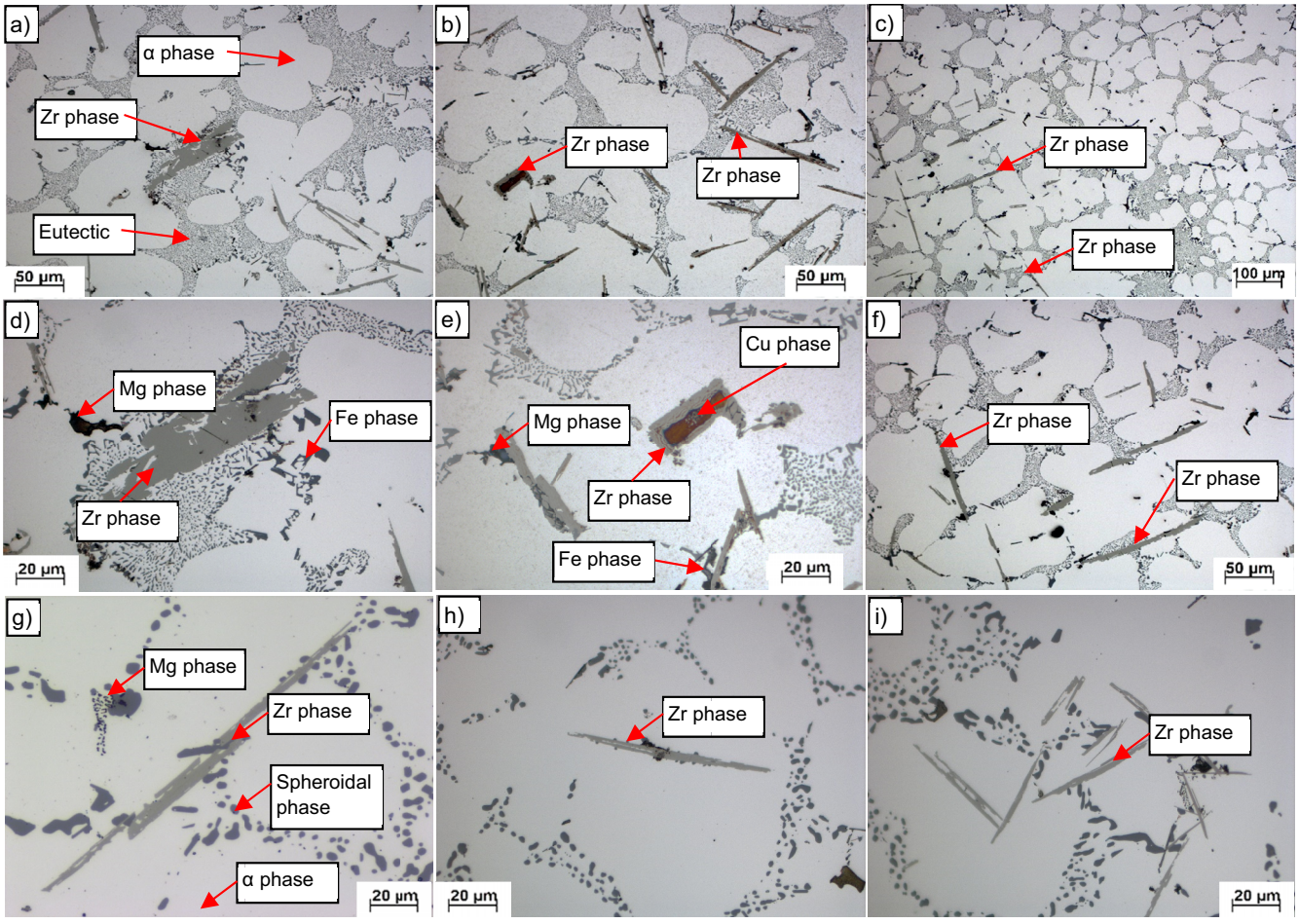

Fig. 10. Microstructure of E1, E2, and E3 alloys before HT: a), d) 0.1 wt.% Ti, b, e) 0.2 wt.% Ti, c, f) 0.3 wt.% Ti.; Microstructure of E1, E2, and E3 alloys after HT: g) 0.1 wt.% Ti, h) 0.2 wt.% Ti, i) 0.3 wt.% Ti, H_2SO_4 etch

remove them from solution forming intermetallic phases and reducing their growth restriction activity [23]. Finally, there is also reported the poisoning effect of Si on grain refinement performance in Al-based alloys containing more than 2-5 wt.% Si through binding Ti, and even causing grains coarsening. This is because Si tends to react with Ti to form Ti-rich silicides of large crystallographic misfit with α-Al and can impair the nucleation potencies of Ti-based nucleation substrates [24-26].

4. Conclusions

A decrease in mechanical properties was recorded in ductility, where in the experimental samples ductility exceeded the values of R alloys. A significant decrease in ductility may be related to an increase in the Zr phase content in the form of longer acicular formations that reduce plasticity of the metal matrix of the experimental AlSi7Mg0.3Cu alloy. The increase in mechanical properties was observed in $Rp_{0.2}$, E and partly also R_m. A significant increase in $Rp_{0.2}$, E and partly also R_m may be related to an increase in the number of Zr phases of smaller dimensions. These increase the strength of the metal matrix while not increasing the brittleness of the metal matrix. The combination of Zr and Ti induces an increase in the number of Zr phases of angular morphology. The most preferred ratio was about 0.25 wt.% Ti. Above the given content, a larger volume of longer acicular formations has been excluded lowering the R_m. Zr phases induced an increase in the interaction between curable Mg_2Si and Al_2Cu phases. At the same time, it was observed Fe interaction with Zr phases occurred. A similar phenomenon was also observed in samples with the addition of Zr only (Fig. 8). On this basis, we can assume the ability of Zr phases to reinforce the metal matrix when binding with curing phases, and reducing negative effect of Fe like corrector. When evaluating the hardness, the most significant increase was in the experimental samples E3. In the evaluation of microhardness, the best values were also measured in samples of E3, in which a higher number of Zr phases was observed without interaction with other phases. This may be related to the increased hardness of the E3 samples because the metal matrix, in addition to the Zr phase content in interaction with other phases, contains an increased number of Zr phases without a given interaction. The mentioned above discussion shows complex aspect of the simultaneous effects of Ti and Zr on the examined Al-Si alloy structure, and detailed elucidation of these effects requires further detailed examinations. Particularly revealing the presence and composition of the mentioned aluminides and silicides should be of interest.

Acknowledgment

The article was written as part of the VEGA 1/0494/17 Grant Agency project. The authors thank the Agency for their support. Our gratitude also goes to Alucast s.r.o. and Nemak Slovakia s.r.o for the technical coverage of experiments.

REFERENCES

[1] E. Tillová, M. Chalupová, Štruktúrna analýza zliatin Al-Si, EDIS, Žilina (2009).
[2] B. Pisarek, P. Rapiejko, C. Szymczak. Arch. Foundry Eng. **137** (17), 1897-3310 (2017).
[3] H. Sandoval, S. Valtiierra. Int. J. of Metalcast. **11** (3), 1939-5981 (2017).
[4] T. Shaokun, L. Jingyuan, Z. Junlong, W. Zhumabieke, L. Dan. J. Mater. Res. Technol. **8** (5), 4130-4140 (2019), DOI: 10.1016/j.jmrt.2019.07.022
[5] D. Bolibruchová, M. Kuriš, M. Matejka. Manuf. J. **49** (11), 552-558 (2018).
[6] F. Wang, D. Qiu, D. Liu, J. Taylor, M. Easton, M. Zhang. Acta Mater. **42** (5), 5636-5645 (2013).
[7] D. Tsivoulas, J. Robson. Acta Mater. **93**, 73-86 (July 2015), DOI: 10.1016/j.actamat.2015.03.057
[8] A.M. Nabawy, A.M. Samuel, F.H Samuel, H.W. Doty. Int. J. Cast Metal. Res. **308** (26), 308-317 (2013). DOI 10.1179/1743133613Y.0000000068
[9] M. Vončina, M. Medved, S. Kores, P. Xie, A. Czeglier, P. Schumacher. Livarski Vestnik **65** (1), 36-48 (2018).
[10] J. Rakhmonov, G. Timelli, F. Bonollo. Mater. Charact. 128, 100-108 (2017), DOI: https://doi.org/10.1016/j.matchar.2017.03.039
[11] M. Medved, S. Kores, M. Vončina, In: Light Metals 373-380 (2018), DOI: 10.1007/978-3-319-72284-9_50
[12] J. Li, H. Oberdorfer, B. Wurster, J. Mater. Sci. **49** (17), 5961-5977 (2014).
[13] B. Baradarani, R. Raiszadeh, Mater. Des. **32** (2), 935-940 (2011).
[14] R. Podrocká, D. Bolibruchová, Arch. Foundry Eng. **17** (3), 2299-2944 (2017).
[15] E. Fischer, C. Colinet, J. Phase Equilib. Diffus. **36** (5), 1547-7037 (2015).
[16] J. Hernandez-Sandoval, A.M. Samuel, S. Valtierra, F.H. Samuel. Int. J. Metalcast. **11**, 428-439, (2017), DOI: 10.1007/s40962-016-0080-0
[17] D. Bolibruchová, D. Richtárek, S. Dobosz, K. Major-Garyś, Arch. Metall. Mater. **62** (1), 1733-3490 (2017).
[18] Ch. Fuller, D. Seidman, D. Dunand, Acta Mater. **52** (11), 4803-4814 (2003).
[19] W.K. Krajewski, J. Buraś, P.K. Krajewski, A.L. Greer, K. Faerber, P. Schumacher, Mater. Today: Proc. **2**, 4978-4983 (2015).
[20] W.K. Krajewski, A.L. Greer, J. Buraś, G. Piwowarski, P.K. Krajewski. Mater. Today: Proc. **10**, 306-311 (2019).
[21] A. Kozlov, R. Schmid-Fetzer. IOP Conf. Series: Materials Science and Engineering **27** (2011) 012001, doi:10.1088/1757-899X/27/1/012001
[22] A.M. Bunn, P. Schumacher, M.A. Kearns, C.B. Boothroyd, A.L. Greer. Mater. Sci. Technol. **15**, 1115-1123 (1999).
[23] J.A. Spittle, S.B. Sadli. Cast Met. **7**, 247-253 (1994).
[24] D. Qiu, J.A. Taylor, M.-X. Zhang, P.M. Kelly. Acta Mater. **55**, 1447-1456 (2007).
[25] Yang Li, Bin Hu, Qinfen Gu, Bin Liu, Qian Li. Scripta Mater. **160**, 75-80 (2019).
[26] Yang Li, Bin Hu, Bin Liu, Anmin Nie, Qinfen Gu, Jianfeng Wang, Qian Li. Acta Mater **187**, 51-65 (2020).